International Journal of Pharmaceutics: X 6 (2023) 100221

Contents lists available at ScienceDirect

International Journal of Pharmaceutics: X

journal homepage: www.sciencedirect.com/journal/international-journal-of-pharmaceutics-x

# Exploring high-throughput synchrotron X-Ray powder diffraction for the structural analysis of pharmaceuticals

M. Reinle-Schmitt [a], D. Šišak Jung [b], M. Morin [a], F.N. Costa [a], N. Casati [c,*], F. Gozzo [a,*]

[a] Excelsus Structural Solutions (Swiss) AG, PARK INNOVAARE, 5234 Villigen, Switzerland
[b] DECTRIS, Täfernweg 1, 5405 Baden-Dättwil, Switzerland
[c] Paul Scherrer Institute, Forschungsstrasse 111, 5232 Villigen PSI, Switzerland

ARTICLE INFO

*Keywords:*
X-ray powder diffraction
Synchrotron
High-throughput
Beamline automatisation
Polymorphism

ABSTRACT

Synchrotron radiation offers a host of advanced properties, surpassing conventional laboratory sources with its high brightness, tunable phonon energy, photon beam coherence for advanced X-ray imaging, and a structured time profile, ideal for capturing dynamic atomic and molecular processes. However, these benefits come at the cost of operational complexity and expenses. Three decades ago, synchrotron radiation facilities, while technically open to all scientists, primarily served a limited community. Despite substantial accessibility improvements over the past two decades, synchrotron measurements still do not qualify as routine analyses. The intrinsic complexity of synchrotron science means experiments are pursued only when no alternatives suffice. In recent years, strides have been made in technology transfer offices, intermediate synchrotron-based analytical service companies, and the development of high-throughput synchrotron systems at various facilities, reshaping the perception of synchrotron science. This article investigates the practical application of synchrotron X-Ray Powder Diffraction (s-XRPD) techniques in pharmaceutical analysis. By utilizing concrete examples, we demonstrate how high-throughput systems have the potential to revolutionize s-XRPD applications in the pharmaceutical industry, rapidly generating XRPD patterns of comparable or superior quality to those obtained in state-of-the-art laboratory XRPD, all in less than 5 s. Additional cases featuring well-established pharmaceutical active ingredients (API) and excipients substantiate the concept of high throughput in pharmaceuticals, affirming data quality through structural refinements aligned with literature-derived unit cell parameters. Synchrotron data need not always be state-of-the-art to compete with lab-XRPD data. The key lies in ensuring user-friendliness, reproducibility, accessibility, cost-effectiveness, and the streamlined efforts associated with synchrotron instrumentation to remain highly competitive with their laboratory counterparts.

## 1. Introduction

### 1.1. Synchrotron and laboratory XRPD for pharmaceutical applications

The X-Ray Powder Diffraction technique, which has its roots in the early 20th century (Debye and Scherrer, 1916; Hull, 1917), has rapidly become a widely accepted and popular method for analyzing crystalline materials. Its non-destructive nature and ability to analyze a diverse range of materials has led to its widespread use in various fields, such as materials science, chemistry, geology, biology, and pharmacy. The development of X-ray diffraction laboratory equipment that can easily and routinely obtain suitable diffraction patterns from powders has greatly contributed to its popularity and widespread use in research and industry. In the past two decades, the development of advanced instrumentation (Bergamaschi et al., 2010; Abdellatief et al., 2022; Dejoie et al., 2018; Vanmeert et al., 2018; Thomae et al., 2019; Artioli et al., 2015; Vaughan et al., 2020) and methodologies (Halasz et al., 2013a; Spiliopoulou et al., 2021; Newman et al., 2015) as well as software development (Juhas et al., 2013; Degen et al., 2014; Toby and Von Dreele, 2013; Coelho et al., 2011; Petříček et al., 2014; Filik et al., 2017) and database content (Gates-Rector and Blanton, 2019) has dramatically changed the impact of XRPD in science (Jenkins, 2001), and XRPD is no longer just a technique for routine assessments, but a powerful tool for the structural and microstructural analysis of materials. Initially addressing polycrystalline materials only, XRPD analytical applications also extended to the study of poorly crystalline and non-crystalline

* Corresponding authors.
*E-mail addresses:* nicola.casati@psi.ch (N. Casati), fabia.gozzo@excelsus2s.com (F. Gozzo).

https://doi.org/10.1016/j.ijpx.2023.100221
Received 11 July 2023; Received in revised form 20 November 2023; Accepted 27 November 2023
Available online 29 November 2023

materials with the application of so-called total scattering techniques (e.g. Pair Distribution Function, Debye model) that interpret both Bragg and diffuse scattering and allow us to access the local structure of materials (Terban and Billinge, 2022; Giannini et al., 2007). Dealing with powders as opposed to single crystals, makes XRPD ideal for in-situ and *in-operando* studies and recent development of fast X-Ray detectors (Bergamaschi et al., 2010; Šišak Jung et al., 2017; Donath et al., 2023) have unlocked the access to the kinetics of phase transformations and the study of phenomena under non-ambient conditions (Stolar et al., 2019; Hocine et al., 2020).

In pharmaceutical science, XRPD also stands out as a pivotal technique that plays a crucial role in numerous aspects of research and development (Ivanisevic et al., 2010; Byrn et al., 2017; Rodriguez et al., 2021). XRPD provides critical support for a wide range of development activities including solid form screening, phase identification and quantification, ab-initio structure solution and/or refinement, microstructure analysis, stability testing and quality control (Gozzo, 2018; Thakral et al., 2018; Billinge, 2015). Furthermore, it supports Intellectual Property (IP) rights protection and is a powerful method to identify counterfeit pharmaceuticals (Musumeci et al., 2011; DeWitt, 2015). Because each crystal form is uniquely identified by its powder pattern, XRPD directly detects and uniquely identifies multiple solid crystal forms of the same pharmaceutical compound making it the gold standard technique for the study of the polymorphism of pharmaceuticals (Bernstein and Reutzel-Edens, 2019).

Due to the complexity of pharmaceutical molecular structures, the polymorphism of pharmaceuticals is a rich and complex phenomenon and XRPD data quality plays a key role: the higher the data quality, the lower the uncertainty of phase identifications.

Lab-XRPD is widely applied in industry for the routine analysis of pharmaceutical compounds. The setup often involves copper Kα X-Ray radiation and linear (1-dimensional, 1D) or area (2-dimensional, 2D) X-ray detectors. Linear detectors installed at laboratory diffractometers often cover a limited 2θ range (ca. 20° in 2θ) and, therefore, require scanning the detector along the 2θ axis to generate a powder diffraction pattern over a workable 2θ range. Lab-XRPD data collection is time consuming and the higher the quality desired of the diffraction pattern the more time consuming the data collection. Modern lab-XRPD are efficiently automatized allowing for unsupervised sequential data collection over a multitude of samples and the reliability and user-friendliness of modern lab-XRPD instrumentation is impressive. Still, a compromise between resolution, signal-to-noise and duration of measurements is indispensable.

The boundaries of adequacy for lab-XRPD are determined by factors such as the complexity of the pharmaceutical compound under investigation, including the number of independent molecules in the unit cell and the degrees of freedom within the molecular structure, as well as the desired Limit of Detection (LOD) and Quantitation (LOQ). Additionally, considerations of the timescale of the observed phenomenon come into play. When aiming for LOD/LOQ levels below 0.1%, fast data acquisition, and angular resolutions of the order of a few millidegrees, it becomes worthwhile to explore s-XRPD and its potential to strike a balance with the compelling reasons that lead us to synchrotrons, rather than being seen merely as a 'last resort' solution. The question then arises: will the adoption of high-throughput s-XRPD transform it into a powerful routine facility?

Owing to the extraordinary properties of synchrotron radiation, s-XRPD dramatically enhanced the overall quality of XRPD analysis. Among the many properties that make synchrotron radiation a powerful source of electromagnetic radiation, high-brilliance (i.e. high photon beam intensity in a small and parallel beam) and tunability of the photon energy over a continuous and wide interval are those that mostly contribute to the outstanding quality of s-XRPD data in terms of high angular resolution and signal-to-noise ratios.

Just like lab-XRPD, s-XRPD proves useful for a wide range of tasks in pharmaceutical sciences. As mentioned above, s-XRPD is ideal to tackle very difficult problems for which the access to superior data quality and/or complex experimental setups is instrumental: ab-initio structure determination (Grässlin et al., 2013; Šišak Jung et al., 2014); extremely low detection limits (Gozzo, 2018); mapping of crystalline and amorphous content (Ditzinger et al., 2019); and following fast and complex solid-state transformations (Halasz et al., 2013b).

### 1.2. S-XRPD high-throughput systems

In the past 20 years, access to synchrotron sources has been largely facilitated and the user-friendliness of synchrotron instrumentation has reached levels that allow non-experts to access the facilities as in the past would not have been possible. S-XRPD for routine measurements is now conceivable and therefore, next to pharmaceutical applications addressing problems that are of extraordinary difficulty requiring temporal-, angular- and/or spatial- resolution through novel and outstanding methodologies, a new gate opens that can democratize the use of s-XRPD technique via an easier and routine access to beamlines, made possible by the development of efficient *high throughput* experimental setups.

The demand for high-throughput measurements is arising from multiple sources. Firstly, businesses that generate large sample volumes have traditionally faced challenges in analyzing them due to technical limitations. Examples include geological surveys and mining industries. Secondly, even when samples to test are not too many, the analysis of a sub volume of each sample may not provide sufficient representativeness, especially since standard diffraction measurements typically involve amounts of materials below 100 mg. Multiple samples may therefore need to be collected to access more representative volumes of sample. Thirdly, advancements in science and technology are driving the utilization of large-scale data for predictive modeling and comprehensive understanding of complex systems and materials requiring building training sets and database for machine learning. Finally, s-XRPD high-throughput measurements will eventually result in competitive costs per measurement when dealing with significant number of samples. It is not far-fetched to anticipate a future where even quality control units require continuous access to such large-scale facilities.

In a high-throughput system, two key factors require attention: prioritizing time-efficient data collection and optimizing the entire data handling process, including sample preparation, measurement, analysis, and result generation. In this context, the management of samples and data takes precedence over the cost of beamtime.

Streamlining sample preparation protocols becomes of paramount importance. This involves avoiding sample grinding, simplifying sample placement in the holder, and establishing an unambiguous connection between each sample holder and its corresponding sample. In 2017, initial concepts were developed at the SLS to address the challenges posed by large sample quantities. This approach involved utilizing metal plates with numerous holes sealed on both sides, allowing for rapid sample changes by moving from one hole to the next. However, this approach neglected the complexities of sample loading and the need to establish a precise correlation between each position and a specific sample, thereby introducing the potential for human error.

Powder holders are usually subjected to rotation, spinning, or movement to enhance the statistical distribution of powder crystallite orientations during measurements. In line with this common practice, our second-generation high-throughput system was intentionally designed with this requirement in mind from its inception. In its first version, our system implemented a combination of small plate translations and gentle rocking of the plate itself, which helped partially alleviate the issue. Fig. 1 shows a portion of Debye Scherrer rings collected on a granular and highly oriented natural geological powder mixture. Starting from the center, which is the origin of the reciprocal (diffracted intensities) space, Debye Scherrer rings picture bi-dimensional diffraction patterns. Each ring represents a family of

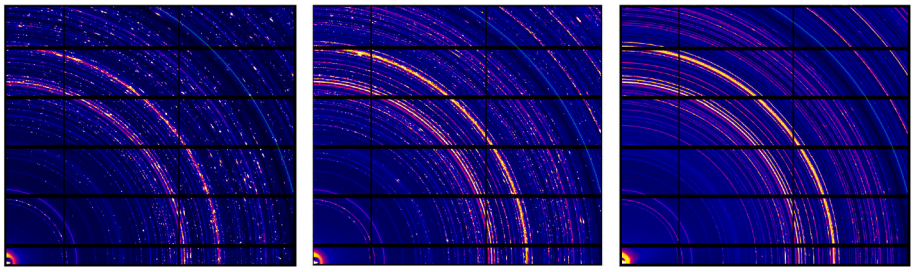

**Fig. 1.** Data collected without sample movement (Left) produce grainy diffraction arcs, with lower representativeness of the final integrated data. Rocking and translating the sample (Center) produces a substantial improvement and an acceptable compromise. Only an optimal randomization of the powder crystallites produces Debye-Scherrer rings that are spotless with diffracted intensity uniformly distributed along the rings' circumference (Right).

crystallographic planes at a given 2-theta angle or merge of families of crystallographic planes with same or close d-spacings. In an ideal powder, the diffracted intensity is uniformly distributed along each ring and data collection across any radial direction would generate the same identical 1-dimensional diffraction pattern (*Intensity*-versus-*2-theta)*. Spottiness in such Debye-Scherrer rings is equivalent to a non-statistical representation of the crystallites in the powder sample due to a poor statistic of orientation of the powder crystallites and/or to crystallographic planes preferentially oriented with respect to others. In Fig. 1, we easily appreciate how the rings evolve from very spotty (Fig. 1, Left), where the sample was kept still during data collection, to partly continuous (Fig. 1, Center), where sample rocking and translation was applied, hence improving the randomness of the orientation of the powder crystallites. Fig. 1, Right shows how the Debye-Scherrer rings look like with optimum randomization of the powder crystallites, i.e. spotless and with uniform distribution of diffracted intensity along the rings' circumference. The integration of the intensity along the rings generates 1-dimensional *Intensity*-versus-*2-theta* powder patterns, which are in fact 1D projections of 2D images of the kind shown in Fig. 1. It should be noted that, an experimental setup capable of appropriate randomization of powder crystallites allows one to collect data corresponding to just one quadrant of the Debye-Scherrer rings and hence extend the value of the maximum 2-theta value reached.

In 2020, scientists at the European Synchrotron Radiation Facility (ESRF) in Grenoble, France, in collaboration with an industrial partner and with funding from the European Commission (*Streamline project: New high-throughput X-ray powder diffraction system on ID*31, 2023), launched a high-throughput system tailored specifically for battery research applications conceived as a system with a reliable sample tracking system via a QR code and a gentle shaking of the powder that improved the quality of the diffraction pattern obtained.

In this article, we present and discuss the latest development of XRPD high-throughput systems developed and commissioned at the Swiss Light Source (SLS) Materials Science Powder Diffraction (MS-PD) beamline (Willmott et al., 2013) and provide a demonstrative application of high-throughput s-XRPD applied to pharmaceuticals with the analysis of atorvastatin calcium trihydrate, which is the API in the Lipitor® drug, commercially available as a certified reference compound. Atorvastatin s-XRPD patterns recorded with the SLS MS-PD high-throughput system are compared with (i) lab-XRPD data collected using good laboratory instrumentation and (ii) routine lab-XRPD patterns published in the US WO 03/004470 A1 patent (Byrn et al., 2003). To strengthen the concept of high throughput applied to pharmaceuticals, we also discuss the application of high throughput s-XRPD to several additional pharmaceutical compounds. The quality of patterns is further consolidated by partial structure refinements against the known crystallographic unit cell of the compounds we considered.

## 2. Methods and materials

A certified pharmaceutical compound, the atorvastatin calcium trihydrate powder, was selected for our study, which is the API in Lipitor® drug products as well as a collection of known and easily accessible pharmaceutical APIs: salicylic acid, cinnarizine and paracetamol and two excipients commonly used in formulations: lactose monohydrate and sorbitol.

The following pharmaceutical powders were purchased from the company Merck-Sigma Aldrich: atorvastatin calcium trihydrate ($C_{66}H_{68}CaF_2N_4O_{10}{\cdot}3H_2O$) is product number Y0001327 – CAS No. 344423–98-9, European Pharmacopoeia (EP) Reference Standard. Salicylic acid (2-(HO)$C_6H_4CO_2H$) is product number 247588 – CAS No. 69–72-7, paracetamol ($CH_3CONHC_6H_4OH$) is product number A7085 – CAS 103–90-2 and Sorbitol ($C_6H_{14}O_6$) is product number PHR1006 – CAS 50–70-4. Lactose monohydrate ($C_{12}H_{22}O_{11}H_2O$) was purchased from the company VWR and its product number is 20D214119 – CAS 10039–26-6. Cinnarizine was kindly donated by Novartis Pharma AG.

Powders were all loaded in individual holder ('washers') in a closed glove box at controlled temperature (22 ± 2 °C) and ambient relative humidity up to an optimum tapped volume of 50%. With the term 'tapped volume' we refer to the volume that results after gently 'tapping' the washer to consistently compact the powder.

All s-XRPD datasets were recorded at the SLS MS beamline, at a nominal photon energy of 17.5 keV using a Pilatus 6 M area detector. The wavelength was calibrated via the refinement of the diffraction pattern of the SRM640d standard from NIST (for atorvastatin: 0.70793 (1) Å, for salicylic acid/cinnarizine/paracetamol: 0.70828(1) Å, for lactose/sorbitol: 0.70805(1) Å), and the s-XRPD patterns converted to copper Kα wavelength of 1.54056 Å for comparison with the patent and high-resolution lab-XRPD patterns on a 2θ scale. The beam was focused to about 90 × 180 microns (Full Width at Half Maximum, FWHM) and then further restricted in size by means of a circular pinhole with a diameter of 150 μm.

S-XRPD patterns of atorvastatin calcium trihydrate API, lactose monohydrate and sorbitol were collected via the newly developed high-throughput system of the SLS-MS beamline described in this article, with a shaking frequency of 50 Hz in runs of 3 s. S-XRPD patterns of salicylic acid, cinnarizine and paracetamol via the high-throughput system further developed by ANAXAM. The detector-to-sample distance was calibrated with s-XRPD patterns collected on $LaB_6$ samples. Integration of the 2D images collected with the Pilatus 6 M detector to 1D s-XRPD patterns was performed with Dioptas (Prescher and Prakapenka, 2015) software.

A high-resolution lab-XRPD pattern was recorded at the Small Molecule Crystallography Center (SMoCC) at the Swiss Federal Institute of Technology in Zurich (ETHZ) on the same powder analyzed with the SLS high- throughput system for a straightforward comparison. For high-resolution lab-XRPD measurements, powder was loaded in 0.8 mm borosilicate glass capillary and data collected for 12.5 h using the 1-dimensional single-photon-counting solid-state silicon MYTHEN detector.

Pawley refinements were performed using TOPAS® software (Bruker, 2016).

## 3. Resultsanddiscussion

### 3.1. The latest optimized SLS-MS high-throughput system

A substantial improvement of the SLS-MS high throughput system was achieved when we adopted a completely different approach. Inspiration came from the CheMin instrument of NASA's Discovery mission (Blake, 2023). This approach utilized a piezo motor to shake the plates, ensuring continuous movement of the powders and reorientation of the grains. While smaller plates proved necessary, the initial assessment of this technique indicated a highly positive impact on data quality. The Debye-Scherrer rings shown in Fig. 1 (Right image), which we indicated as representing the ideal appearance of diffracted intensity distribution, was obtained with a vigorous shaking movement of the powder that substantially improved the particle statistics. This approach, however, did not fully resolve the complexity associated with sample loading, but it constituted a step forward in addressing the grain statistic issue. The motors used lacked sufficient power to thoroughly mix the materials and the fine movement of the shaking could potentially lead to segregation of finer grains and/or denser ones in the lower portion of the sample holders. This presented a significant challenge, particularly in terms of phase quantification, as the finite beam size only targeted a single position of the sample holder.

The final design solution, whose results we applied to pharmaceutical compounds in this article, involved implementing single *'washer'* holders, consisting of discs each accommodating a single sample. This approach reduced the weight of the material to be shaken, allowing for imparting a strong and vigorous movement to the entire *'washer'* unit. Furthermore, since samples are then prepared independently of any other, the risk of cross-contamination is completely lifted. The stochastic powder shaking of this system leads to optimal grain statistics and minimizes the burden of sample preparation, including the need for extensive grinding. Fig. 2 shows a picture of the system used (Fig. 2, Left) and an exemplified cartoon (Fig. 2, Right). The holders could be easily exchanged within a fixed shaking unit using simple pneumatic translation, enabling rapid sample exchange without the requirement for alignment.

Subsequent developments by ANAXAM (Analytics with Neutrons And X-Rays for Advanced Manufacturing) brought significant engineering enhancements to the initial prototype. The washers were redesigned for user-friendliness, featuring two clipping parts for effortless loading. Additionally, a QR code was integrated onto each washer, enhancing system robustness and reliability while eliminating the need to track the order of washers within the tubes. Instead of tubes, a large funnel was introduced to accommodate the random insertion of washers without the risk of losing track of sample identities, thanks to the QR code identification. The ANAXAM system also includes a QR code reader for seamless operation. The QR code could be scanned during the measurement or at later stages for sample retrieval, thereby avoiding data labeling issues and improving digital operations. These improvements had several advantages, including minimizing sample preparation requirements (i.e. washer's order in the loading tube for sample identification), enabling swift loading, and facilitating immediate digitization of sample IDs.

On the front of data collection strategies, the first step was to determine the minimum exposure time required for a measurement of standard quality, as well as the ancillary time necessary for sample changes and potential alignment. S-XRPD laboratories benefit from substantial photon-flux and advanced detection systems, allowing for ultra-fast measurements. It is, therefore, crucial for these additional steps to be greatly minimized not only to accommodate large number of measurements in relatively short times, but also not to compromise the efficiency offered by s-XRPD with substantial time overheads.

Exposure times for area detectors typically range between 1 and 100 s to obtain high-quality data. While faster measurements are possible, they may result in an unworthy reduction in data quality. The bottleneck for ultra-fast s-XRPD measurements is the time necessary for sample changes and alignment, so unless time is critical for the phenomena to observe, reducing data acquisition time below 1 s is not worth. Conversely, longer acquisition times primarily enhance the signal-to-noise ratio and do not significantly impact other vital measurement aspects, such as instrumental resolution or particle statistics. The latter parameter must be carefully considered, as longer acquisitions do not necessarily improve data quality if particles do not assume a statistically significant larger number of positions during the extra allocated acquisition time. For example, in cases where particles rotate on a fixed disk, longer acquisitions may not enhance data quality, as the quality is limited by grain statistics rather than counting statistics. Our final setup, with its vigorous shaking mechanism, enables improved particle statistics, while limitations in data quality are primarily associated with high background or imperfectly calibrated instruments.

Labeling, sorting, and distributing the data become effortless tasks when the data is digitized during the preparation/acquisition step. It allows for the simultaneous loading and collection of samples from multiple users, with automatic sorting and delivery to the respective clients at the end. The volume of generated data can be efficiently

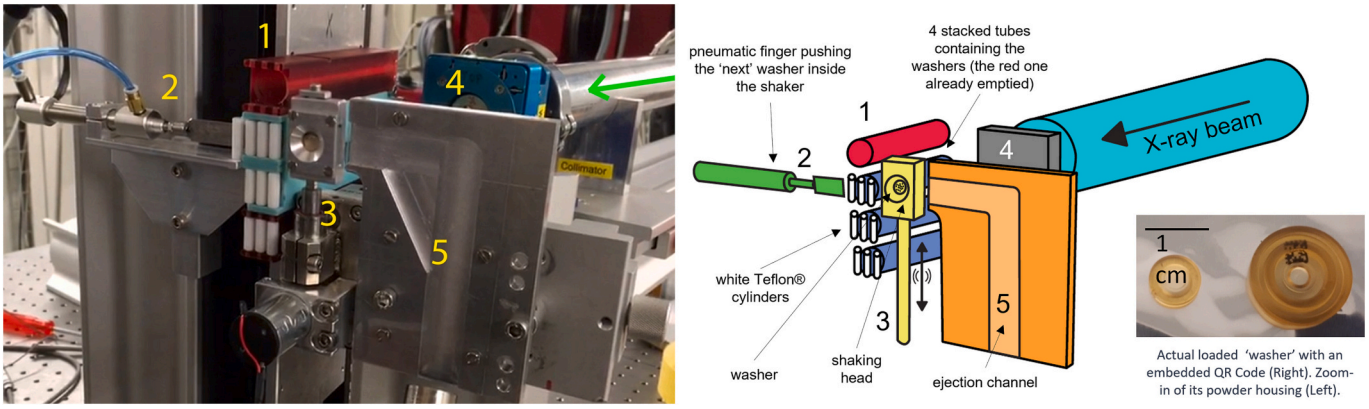


**Fig. 2.** A working prototype for high-throughput exchange system featuring: (1) stacked tubes that hold multiple 'washers' arranged in a specific order. In the image, you can see the top tube in red already empty, while the three bottom ones, which are less visible have their fronts stopped by white Teflon® cylinders. Within each tube, there is a stack of washers, pressed against the Teflon® cylinders. A space between the cylinders and the tube-end enables a (2) pneumatic 'finger' to laterally push the washer from the tube into the (3) shaking head. The shaking head vertically shakes the washer while it is exposed to the X-ray beam coming from (4) the beamline vacuum pipe, before being ejected from the system through a (5) channel. The green arrow shows the X-ray beam direction inside the beamline vacuum pipe.

managed using standard computing resources. However, it is important to note that data analysis remains the most complex and distinctive aspect of each project. It is not the purpose of this article to discuss this aspect.

### 3.2. Comparing Lab-XRPD and high throughput s-XRPD

Can the availability of high-throughput systems at synchrotron facilities transform s-XRPD from a specialized tool for tackling complex challenges in the pharmaceutical industry into a standard destination for routine testing? What prerequisites and additional benefits need to be met to justify the increased migration of lab-XRPD analyses to synchrotron facilities?

We examined this scenario by analyzing a well-studied pharmaceutical compound, the atorvastatin calcium trihydrate powder, which is the API in Lipitor® drug products. S-XRPD high-throughput data were compared with both (i) routine lab-XRPD pattern recorded on nominally the same compound as published in the US WO 03/004470 A1 patent (Byrn et al., 2003); and (ii) high-resolution lab-XRPD pattern recorded on the same powder analyzed with the SLS high-throughput system for a straight-forward comparison.

Fig. 3 shows the lab-XRPD pattern of atorvastatin calcium trihydrate Form IX, as it is described in Fig. 20 of the US WO 03/004470 A1 patent published in 2003.

Patterns of the quality of the one in Fig. 3 are routinely recorded for product registration and patent submissions. Lab-XRPD is, in fact, an accepted methodology commonly used to validate products and spot peaks of the patented form that can uniquely identify it. Data collection of routine lab-XRPD patterns is generally of limited quality, only allowing detection of strong Bragg peaks as it is recorded in acquisition times of the order of an hour. Angular resolution and calibration are poor and signal-to-noise ratio is low, resulting in peak positions quoted in patents with an overall uncertainty of ±0.2° 2θ.

Fig. 4 shows the digitized pattern of atorvastatin calcium trihydrate of the US patent WO 03/004470 A1 PCT/IB02/01796 reported in Fig. 3 (bottom pattern) overlayed with the 12.5 -h high-resolution lab-XRPD powder pattern (middle pattern) and the 3-s s-XRPD pattern (top pattern). The s-XRPD pattern was converted to copper Kα wavelength to directly compare all patterns on a 2θ scale. Fig. 4 (top) shows the overlays of patterns in the entire 2θ range covered in the US WO 03/004470 AI patent, whereas Fig. 4 (bottom) shows details in the restricted 2θ range between 19.8° and 22° 2θ captured by the dotted red rectangle in Fig. 4 (top).

High-resolution lab-XRPD substantially improves the quality of the XRPD pattern. A qualitative inspection of Fig. 4 shows how the high-resolution SMoCC lab-XRPD pattern already displays significant additional details if compared with the routine lab-XRPD pattern published in the 2004 US patent, where we can only identify the main Bragg reflections without appreciating the multiplicity of the diffraction peaks and without detecting diffracted intensity below a threshold. The high-resolution SMoCC lab-XRPD pattern may, however, still not capture all the distinctive features of atorvastatin trihydrate powder, and its lengthy acquisition times are not always compatible with routine testing. In contrast, high-throughput s-XRPD data offers higher resolution and comparable counting statistics in just 3 s. This prompts the question: are the 12.5 h of measurement justified? Is the traditional argument evoking user-friendliness and ease of access of *in-house* lab-XRPD systems still valid?

With the advent of high-throughput systems, the transition to routine use of synchrotron facilities suddenly appears sensible, especially because during the past years synchrotron facilities have been recognizing the importance of providing user-friendly and robust systems, as it is the case at the SLS and at several other synchrotron facilities around the globe.

We also conducted an exercise to explore whether extending the acquisition times at the synchrotron facility would yield any valuable insights within the context of routine qualitative analysis. Fig. 5 shows the same s-XRPD diffraction pattern of atorvastatin in Fig. 4 but collected at increasingly larger acquisition times. In this context of pure routine phase identification, extending the acquisition time to longer than a few seconds does not appear necessary.

To assess the reliability of high-throughput s-XRPD data quality, we conducted supplementary s-XRPD experiments with acquisition times on the order of a few seconds, utilizing well-established pharmaceutical compounds. Additionally, we performed partial structure refinements of all acquired s-XRPD patterns by comparing them against

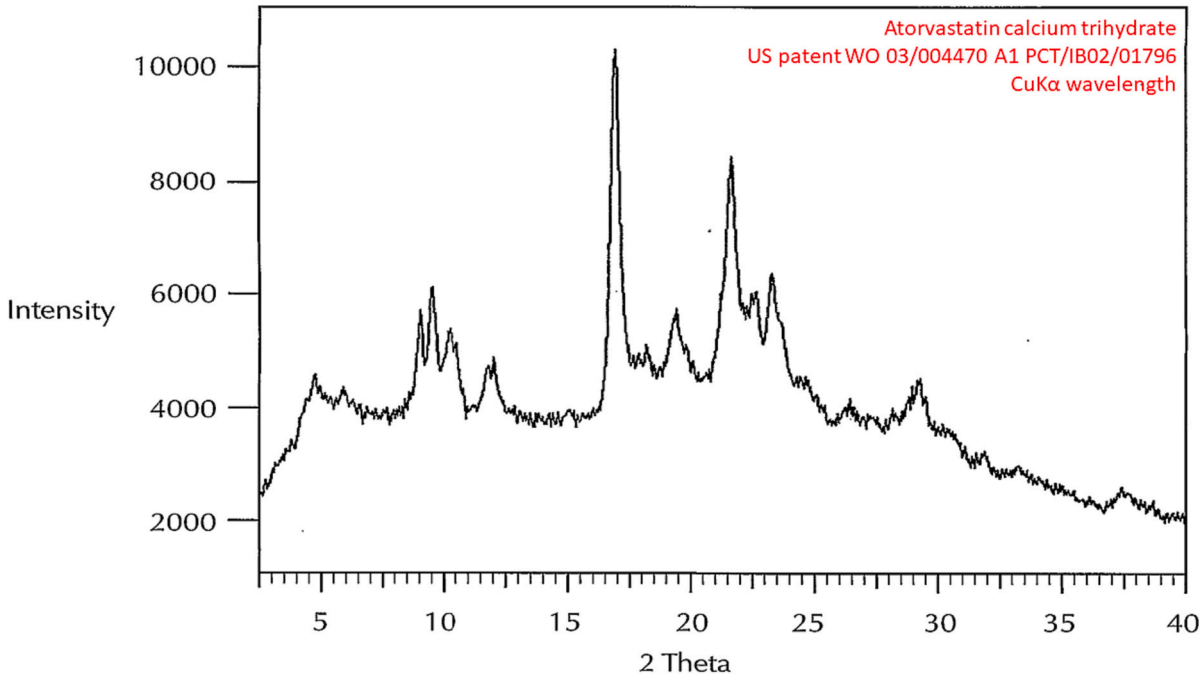


**Fig. 3.** Lab-XRPD pattern of atorvastatin calcium trihydrate, copied from Fig. 20 of the US patent WO 03/004470 A1 PCT/IB02/01796 (Byrn et al., 2003).

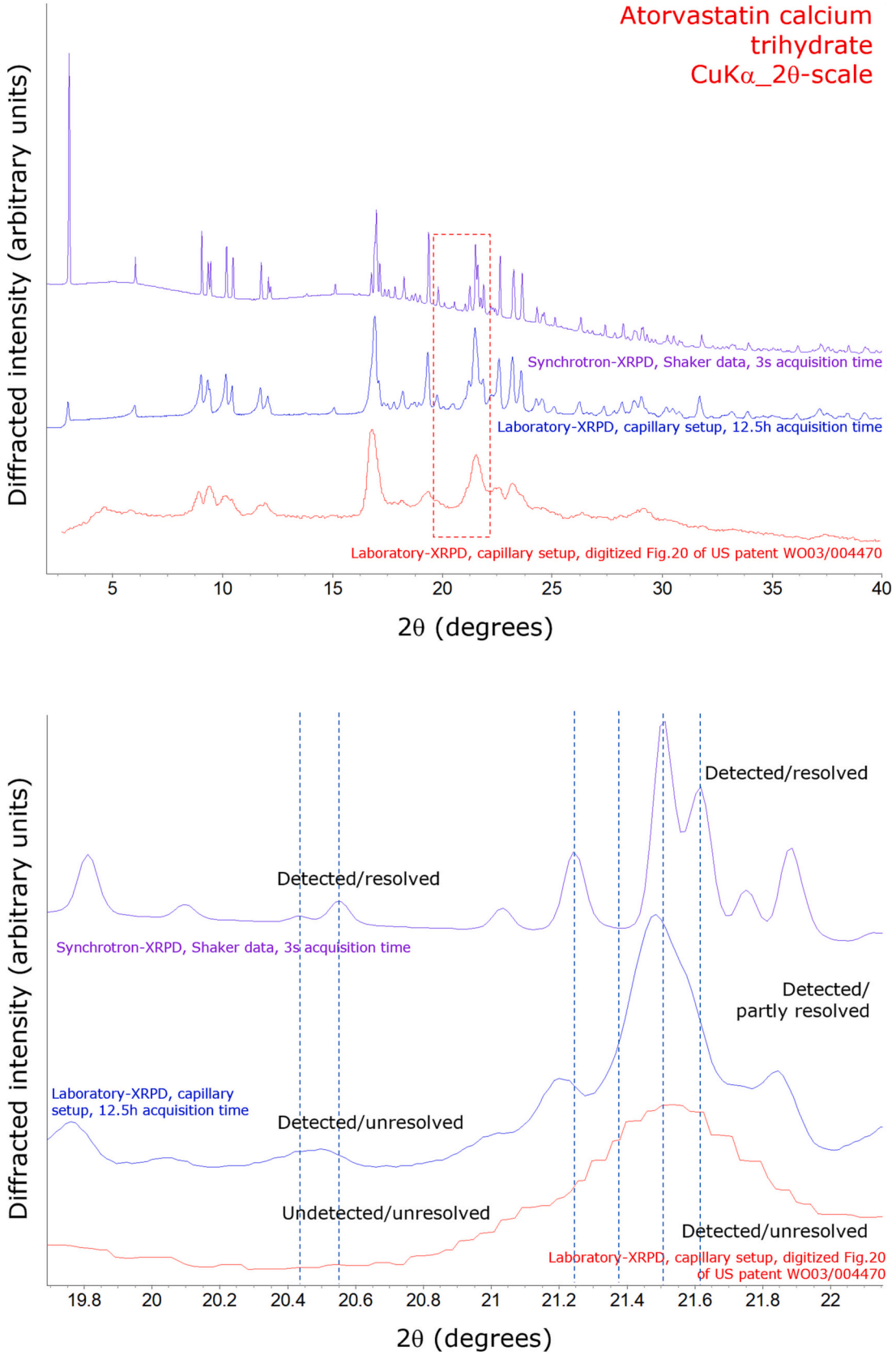


**Fig. 4.** Overlays of atorvastatin calcium trihydrate XRPD patterns featuring the following patterns from bottom to top: digitized pattern from Fig, 20 of the US patent WO 03/004470 (in red); laboratory powder pattern collected with the high-resolution SMoCC lab-XRPD instrument (in blue); s-XRPD patterns collected at the SLS-MS powder station with the high-throughput system described in Section 2a. The synchrotron data were converted to CuKα wavelength for a comparison on a 2θ scale. Patterns have been plotted with a vertical offset to appreciate differences. (For interpretation of the references to colour in this figure legend, the reader is referred to the web version of this article.)

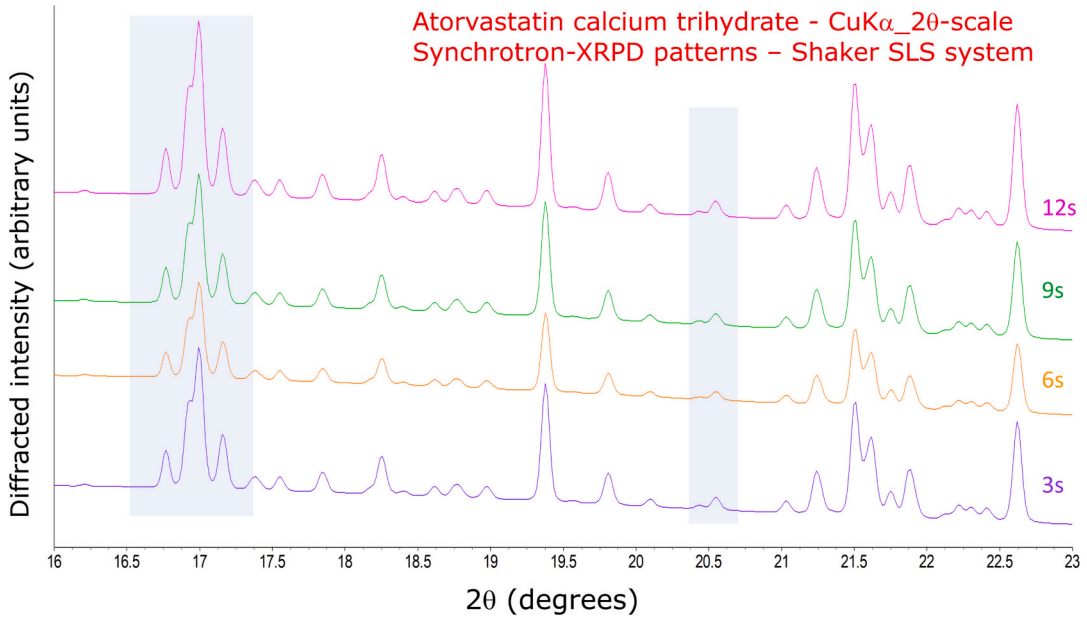


**Fig. 5.** Comparison between atorvastatin calcium trihydrate XRPD patterns collected at 17.5 keV photon energy for 3, 6, 9 or 12 s at the SLS synchrotron with the high-throughput shaker system described in Section 2a. Diffracted intensity is normalized to exposure time and the 2-theta scale converted to copper Kα for a straightforward comparison with the lab-XRPD data. Patterns are shifted along the intensity axes for ease of inspection.

crystallographic data available in the literature (Hodge et al., 2020; Sundaralingam and Jensen, 1965; Mouille et al., 1975; Stone et al., 2009;Rukiah et al., 2005;Smith et al., 2005). Figs. 6–11 show Pawley (Pawley, 1981) refinements against the published unit cell parameters and space group type of the s-XRPD patterns recorded with our high-throughput system of atorvastatin calcium trihydrate, salicylic acid, cinnarizine, paracetamol, D-sorbitol and lactose monohydrate.

The Pawley refinement has proven to be highly satisfactory for all the s-XRPD high throughput patterns collected, with statistical indicators indicating $R_{wp}$ values consistently below 2. These materials were chosen as they are indicative of the small molecules commonly encountered in drug development pipelines.

There is, however, an important aspect that needs to be worked out at synchrotron facilities that presently makes lab-XRPD the only choice for routine and quality-control applications in the pharma industry: their GMP (Good Manufacturing Process) certification and their full

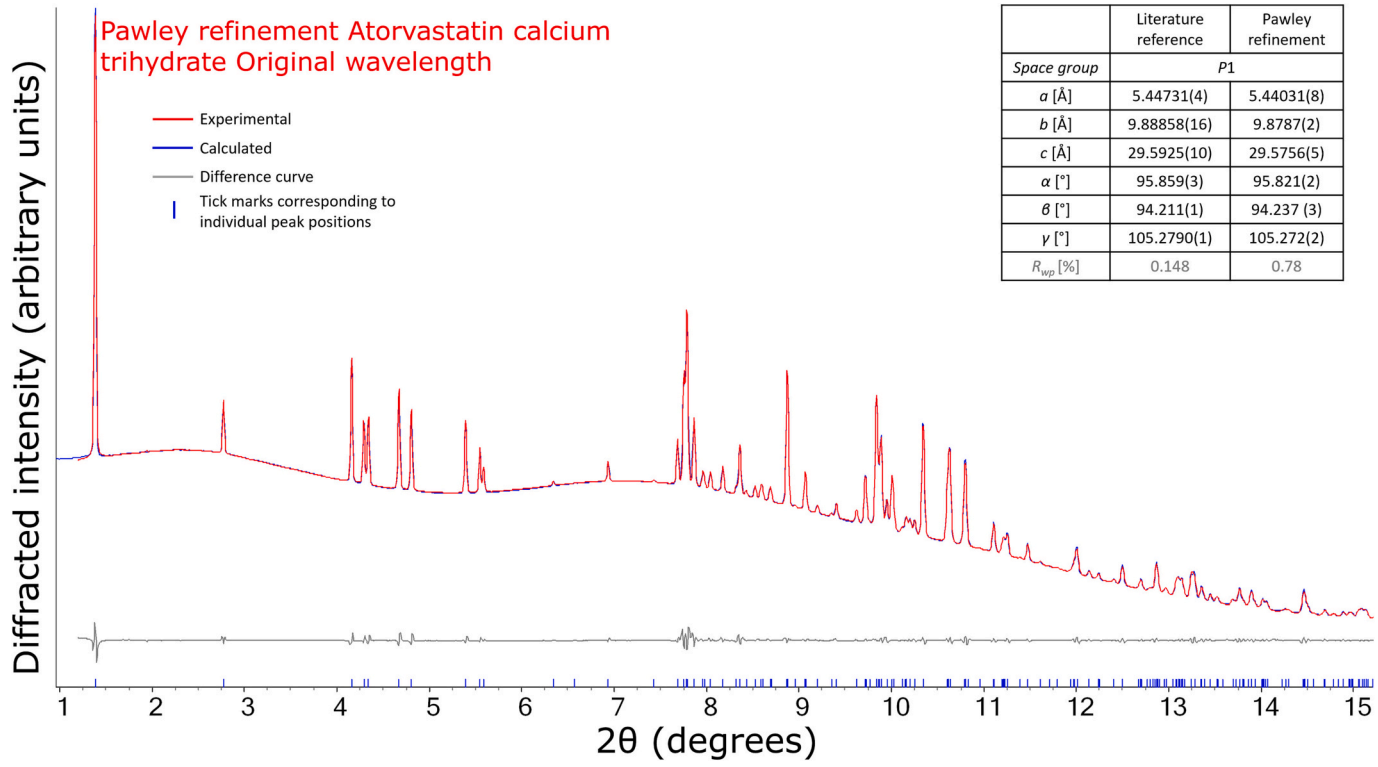


| | Literature reference | Pawley refinement |
|---|---|---|
| *Space group* | *P1* | |
| *a* [Å] | 5.44731(4) | 5.44031(8) |
| *b* [Å] | 9.88858(16) | 9.8787(2) |
| *c* [Å] | 29.5925(10) | 29.5756(5) |
| *α* [°] | 95.859(3) | 95.821(2) |
| *β* [°] | 94.211(1) | 94.237 (3) |
| *γ* [°] | 105.2790(1) | 105.272(2) |
| $R_{wp}$ [%] | 0.148 | 0.78 |

**Fig. 6.** Refinement of the high throughput s-XRPD pattern of atorvastatin calcium trihydrate against the crystallographic unit cell parameters and space group type published in (Hodge et al., 2020).

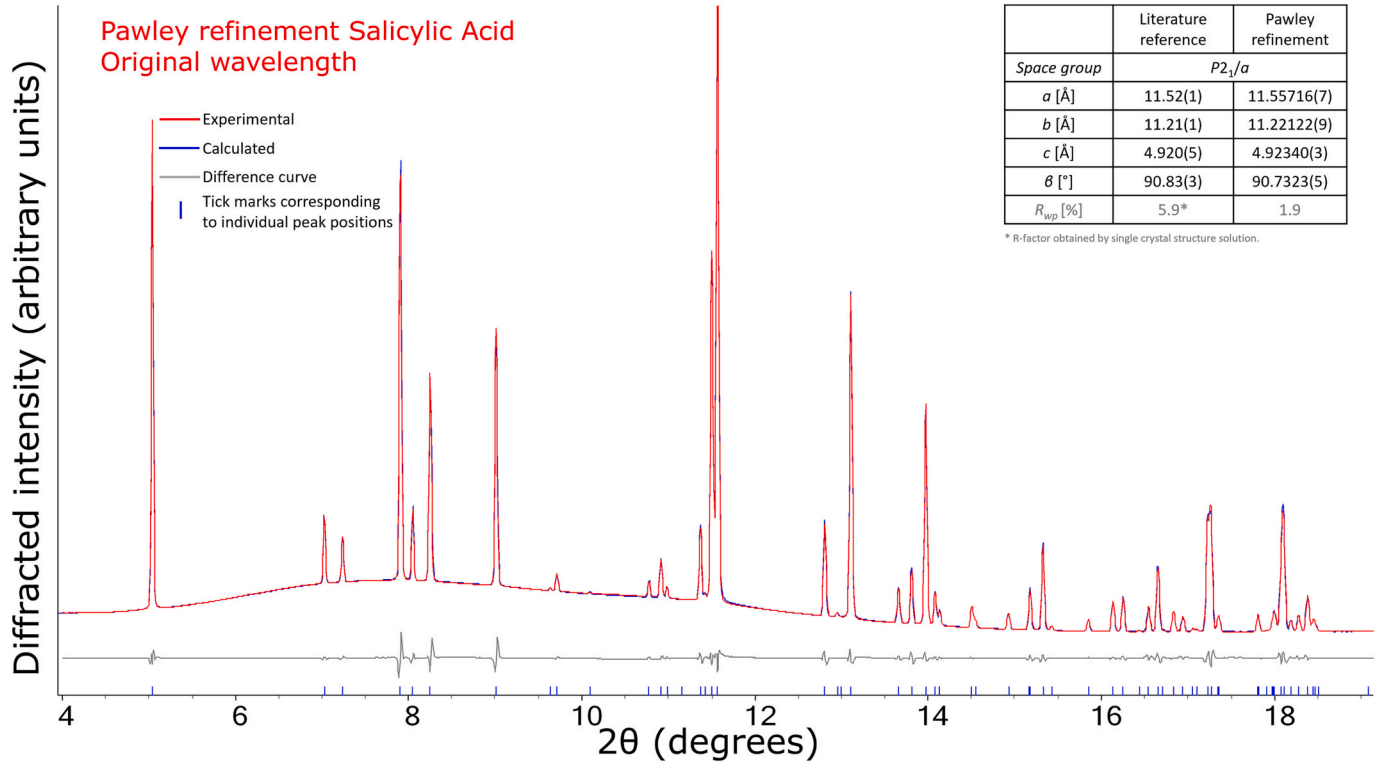


| | Literature reference | Pawley refinement |
|---|---|---|
| *Space group* | $P2_1/a$ | |
| *a* [Å] | 11.52(1) | 11.55716(7) |
| *b* [Å] | 11.21(1) | 11.22122(9) |
| *c* [Å] | 4.920(5) | 4.92340(3) |
| *β* [°] | 90.83(3) | 90.7323(5) |
| $R_{wp}$ [%] | 5.9* | 1.9 |

* R-factor obtained by single crystal structure solution.

**Fig. 7.** Refinement of the high throughput s-XRPD pattern of salicylic acid against the crystallographic unit cell parameters and space group type published in (Sundaralingam and Jensen, 1965).

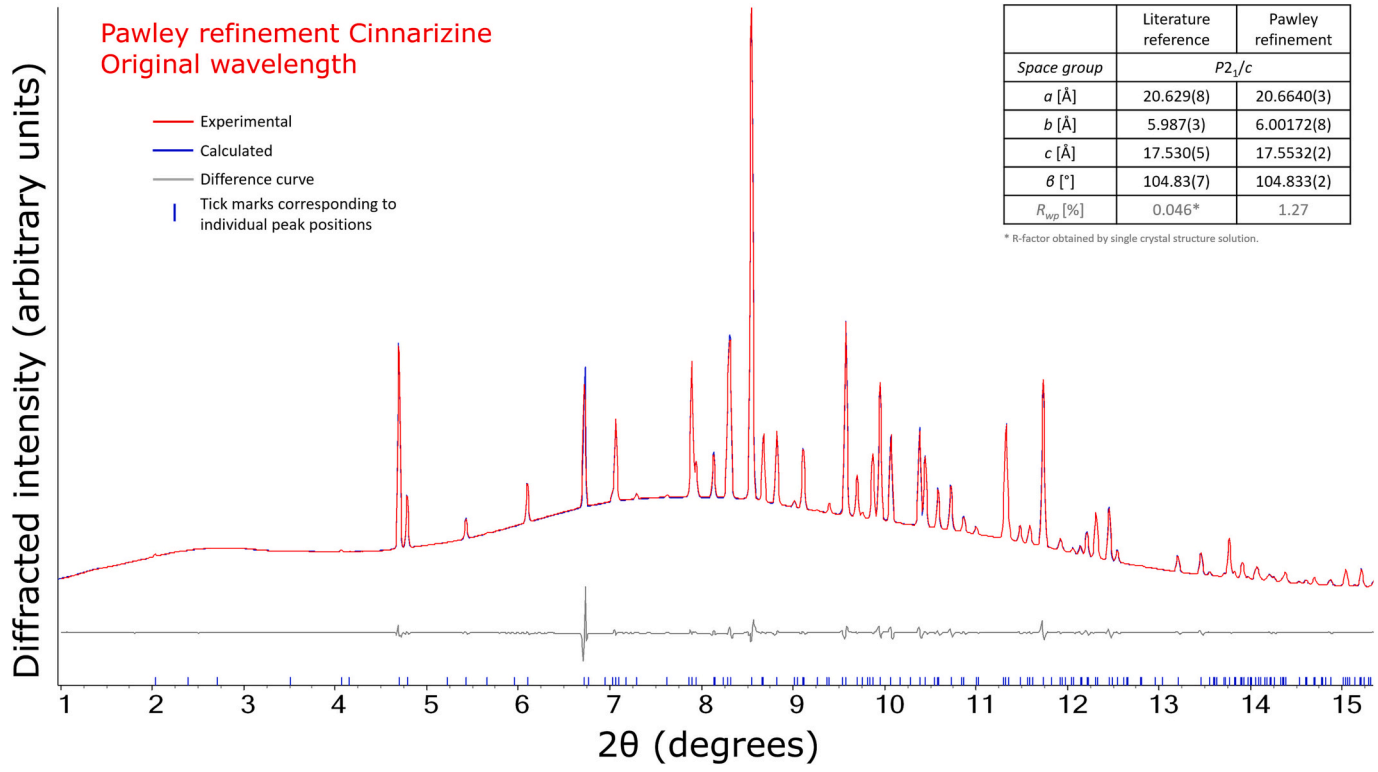


| | Literature reference | Pawley refinement |
|---|---|---|
| *Space group* | $P2_1/c$ | |
| *a* [Å] | 20.629(8) | 20.6640(3) |
| *b* [Å] | 5.987(3) | 6.00172(8) |
| *c* [Å] | 17.530(5) | 17.5532(2) |
| *β* [°] | 104.83(7) | 104.833(2) |
| $R_{wp}$ [%] | 0.046* | 1.27 |

* R-factor obtained by single crystal structure solution.

**Fig. 8.** Refinement of the high throughput s-XRPD pattern of cinnarizine against the crystallographic unit cell parameters and space group type published in (Mouille et al., 1975).

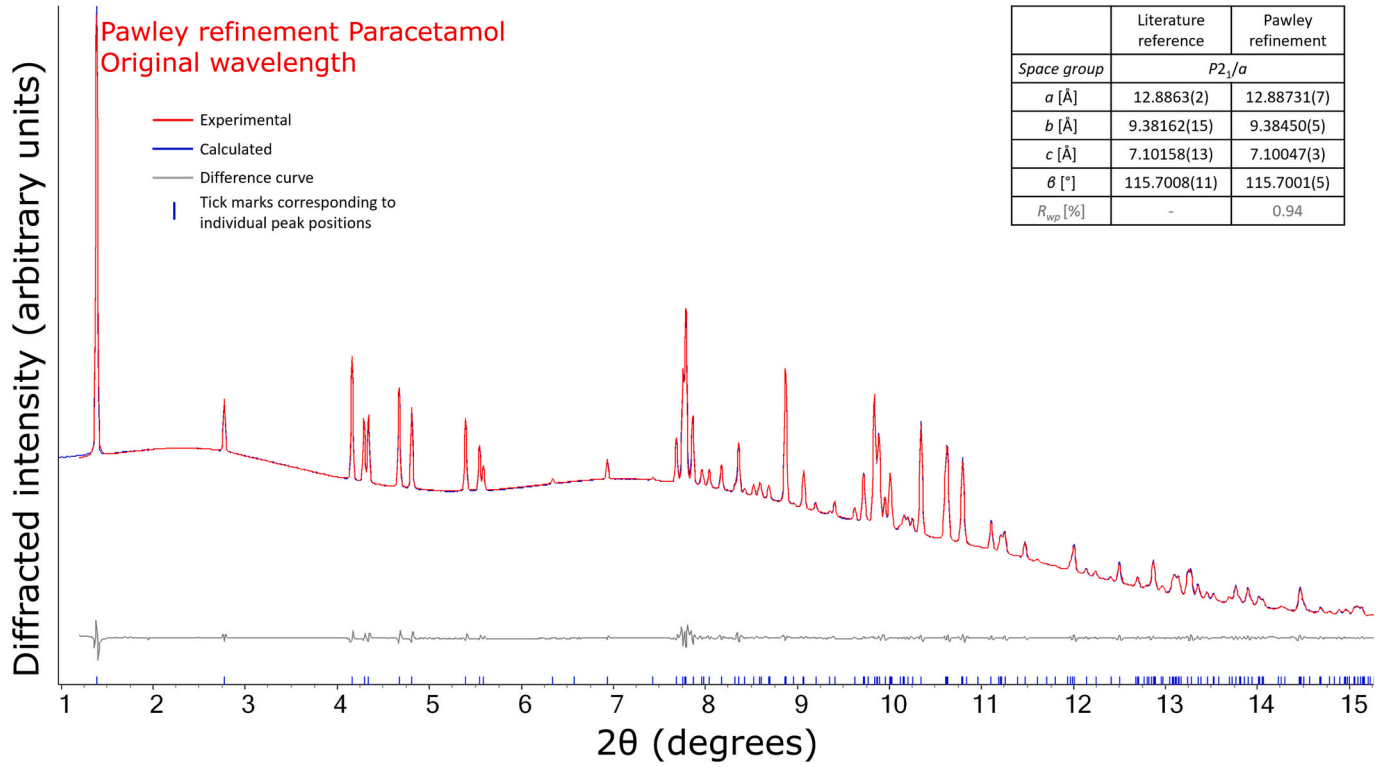


| | Literature reference | Pawley refinement |
|---|---|---|
| *Space group* | $P2_1/a$ | |
| *a* [Å] | 12.8863(2) | 12.88731(7) |
| *b* [Å] | 9.38162(15) | 9.38450(5) |
| *c* [Å] | 7.10158(13) | 7.10047(3) |
| *β* [°] | 115.7008(11) | 115.7001(5) |
| $R_{wp}$ [%] | - | 0.94 |

**Fig. 9.** Refinement of the high throughput s-XRPD pattern of paracetamol against the crystallographic unit cell parameters and space group type published in (Stone et al., 2009).

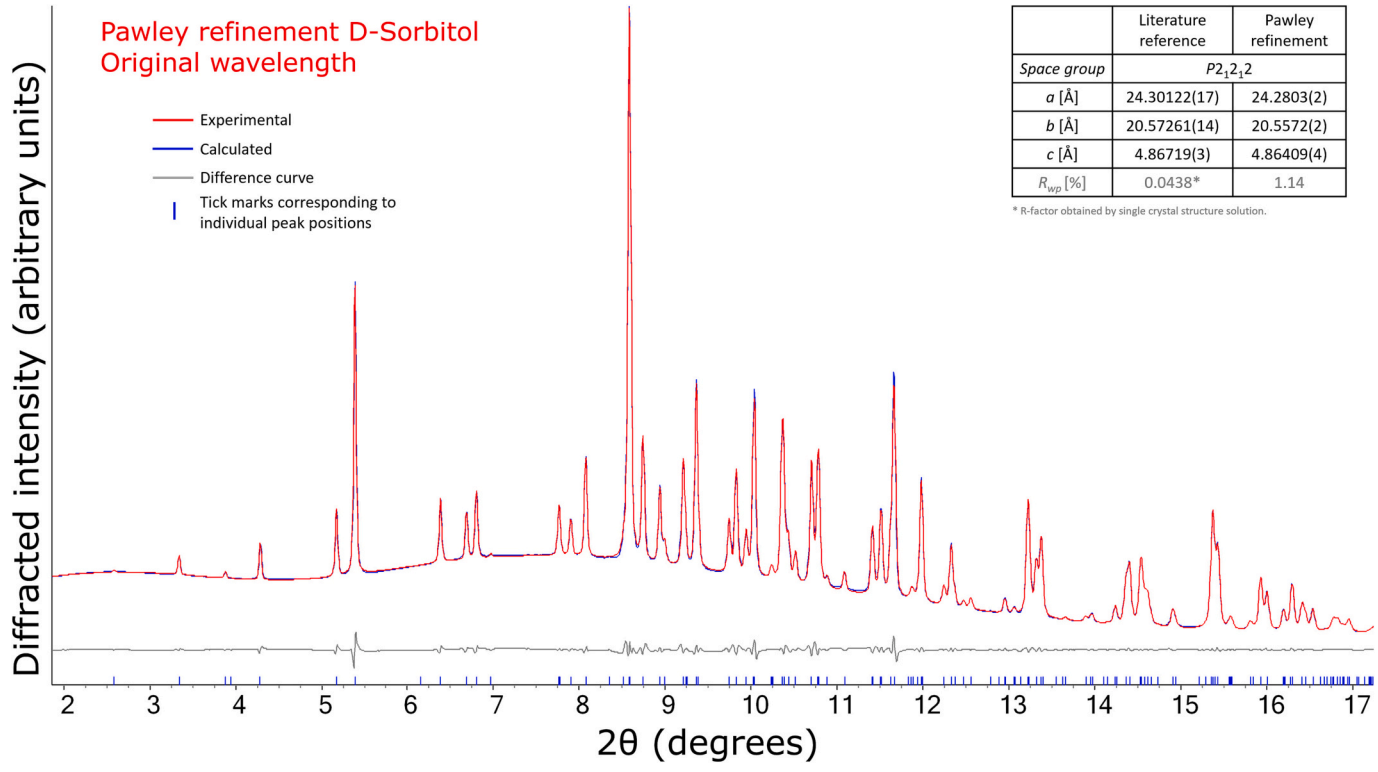


| | Literature reference | Pawley refinement |
|---|---|---|
| *Space group* | $P2_12_12$ | |
| *a* [Å] | 24.30122(17) | 24.2803(2) |
| *b* [Å] | 20.57261(14) | 20.5572(2) |
| *c* [Å] | 4.86719(3) | 4.86409(4) |
| $R_{wp}$ [%] | 0.0438* | 1.14 |

* R-factor obtained by single crystal structure solution.

**Fig. 10.** Refinement of the high throughput s-XRPD pattern of D-Sorbitol against the crystallographic unit cell parameters and space group type published in (Rukiah et al., 2005).

integration into well-established and validated Standard Operating Procedures (SOPs) guaranteeing the compliance with the strict regulatory requirements of the pharma industry. ISO (International Organization for Standardization) certifications are common at laboratory-XRPD instrumentation, not at synchrotron facilities. If working under SOPs or ISO certified is at synchrotron facilities unusual,

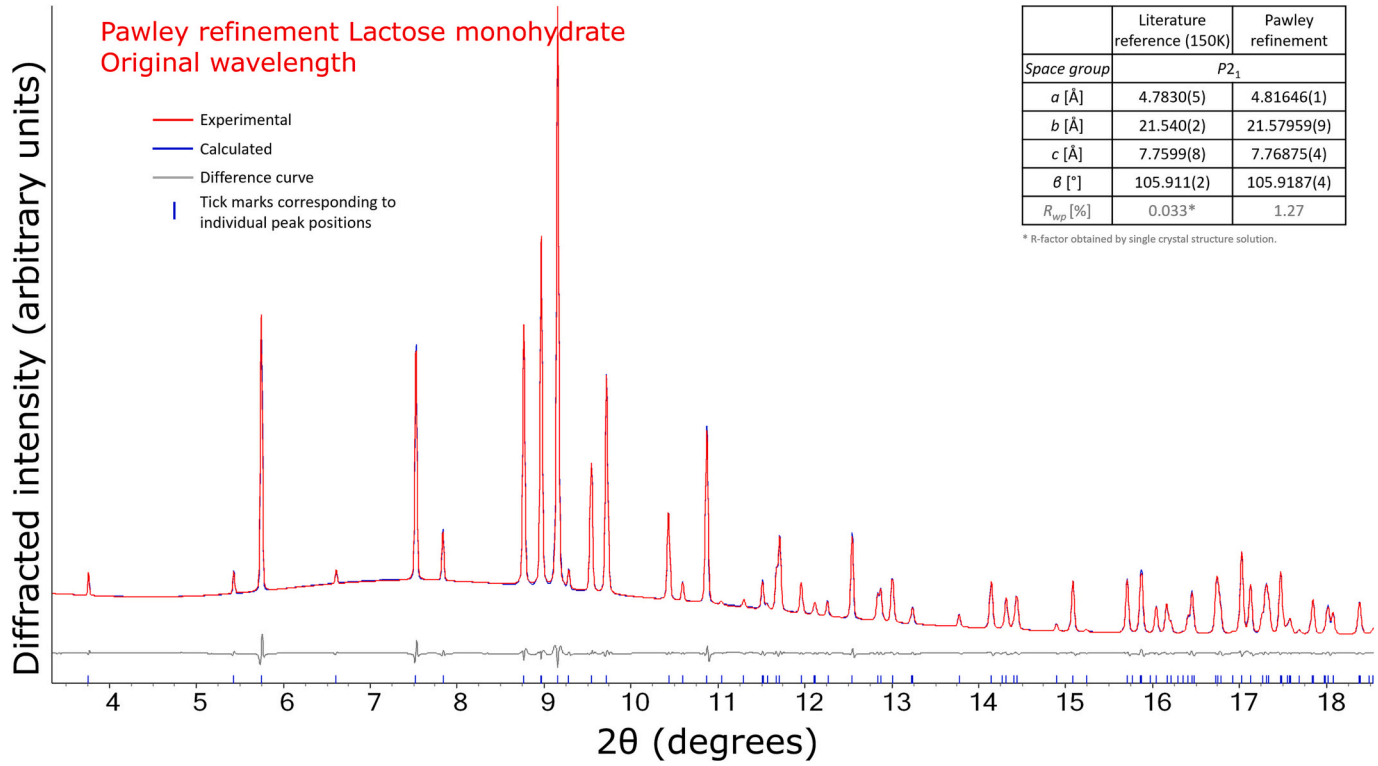


| | Literature reference (150K) | Pawley refinement |
|---|---|---|
| *Space group* | $P2_1$ | |
| *a* [Å] | 4.7830(5) | 4.81646(1) |
| *b* [Å] | 21.540(2) | 21.57959(9) |
| *c* [Å] | 7.7599(8) | 7.76875(4) |
| *β* [°] | 105.911(2) | 105.9187(4) |
| $R_{wp}$ [%] | 0.033* | 1.27 |

* R-factor obtained by single crystal structure solution.

**Fig. 11.** Refinement of the high throughput s-XRPD pattern of lactose monohydrate against the crystallographic unit cell parameters and space group type published in (Smith et al., 2005).

but feasible with the investment of a reasonable amount of resources, working under standard GMP conditions appears a bigger challenge. Working under GMP conditions means that all experimental conditions are rigorously kept unchanged, after having been optimized and validated. A multipurpose powder diffraction beamline will never be able to guarantee that the experimental conditions will be maintained the same and workarounds need to be found. The use of appropriate standard materials to be systematically measured together with the samples under analysis together with the application of robust protocols might be a solution. This might guarantee that data are always collected under the same *nominal* experimental conditions within accepted tolerances. At many synchrotron facilities, metadata have already been enclosed in the headers of datafiles collected with both 1D and 2D patterns, which can be reapplied at every experimental access, and which provides a mean to verify *post-mortem* that experimental parameters were well set. The reduction of XRPD data collected with 2D detectors into *Intensity-versus-2-theta* XRPD patterns is nowadays a routine exercise thanks to the development of efficient, reliable and user-friendly software (Prescher and Prakapenka, 2015; Hammersley, 1997).

## 4. Conclusions and outlook

A new high-throughput system has been meticulously designed and implemented at the SLS-MS, specifically tailored for s-XRPD. This advanced system optimizes not only data acquisition, even in scenarios when preferential orientation and orientation statistics pose challenges, but also enhances sample preparation and exchange procedures. Its primary focus is accelerating and simplifying the entire s-XRPD measurement process. Through a comparison of high-throughput s-XRPD diffraction patterns for the same reference standard of atorvastatin trihydrate with high-resolution lab-XRPD, we were able to perform a valuable assessment of instrument-based performance. Routine high throughput s-XRPD analyses with acquisition times of the order of a few seconds deliver results that are comparable or better than high-resolution lab-XRPD instrumentation lasting several hours. High throughput s-XRPD data performed on multiple reference pharmaceutical powders, followed by partial structural refinements against crystallographic data published in the literature, has also demonstrated that high throughput s-XRPD data maintain a high level of accuracy and reliability.

Significant progress in advancing synchrotron technology, enhancing user-friendliness, improving efficiency, and promoting reproducibility has brought the industrial sector closer to large synchrotron facilities. These improvements have been readily embraced by industry, offering substantial benefits that extend to the academic community as well. While it is important to note that synchrotron-based instrumentation has yet to fully meet the traceability and quality-controlled standards applied in the industrial sector, the development of high-throughput systems within synchrotron facilities is accelerating progress in this direction. Recent instances of synchrotron facilities operating under ISO certifications were highlighted during the inaugural roundtable discussion on certification, validation, and quality assurance at synchrotron facilities, supported by LEAPS INNOVATION (Leaps Innovation, 2023).

Moreover, not all investigations in the pharmaceutical industry require GMP-level rigor; acceptable levels of traceability and reproducibility have already been integrated into synchrotron facilities, often with active involvement from the industrial community.

The next crucial step entails implementing systems across multiple synchrotron facilities to ensure convenient and prompt accessibility for routine studies. Intermediate companies that facilitate access to synchrotron-based techniques also play a pivotal role in reducing the barriers to routinely utilizing synchrotron facilities. The implementation of high-throughput systems demands the development of new and efficient data reprocessing and analysis tools and emphasizes the critical need for robust solutions capable of handling the immense volumes of data involved. In this context, leveraging artificial intelligence becomes paramount, as its capacity to process and make sense of large amounts of

data provides a powerful and indispensable advantage. While lab-XRPD instrumentation will continue to be vital, thanks to the remarkable efforts of XRPD instrumentation manufacturers in producing efficient, user-friendly, and high-quality instruments, its combination with s-XRPD and its wider utilization will be pivotal in advancing the development and characterization of higher quality drugs.

## Credit authors statement

Mathilde Reinle-Schmitt was hands-on with s-XRPD data collection, partial structure refinements, and took the lead in creating the first visual abstract. She also did multiple manuscript reviews.

Dubravka Sisak Jung sparked the idea of writing an article on high-throughput methods and joined in our initial discussions.

Mickael Morin pitched in with s-XRPD data collections and carefully reviewed parts of the manuscript.

Fanny Costa handled all the high-throughput sample prep, helped with s-XRPD data collection, and put together the final version of the visual abstract.

Nicola Casati was the brain behind the Swiss Light Source high-throughput synchrotron-XRPD system prototype and contributed a detailed description of it to the manuscript.

Fabia Gozzo led the project, shaped the manuscript's content, oversaw the s-XRPD measurements, and played a central role in both writing and reviewing it.

## CRediT authorship contribution statement

**M. Reinle-Schmitt:** Formal analysis, Investigation, Writing – review & editing. **D. Šišak Jung:** Resourses, Editing **M. Morin:** Investigation. **F. N. Costa:** Formal analysis, Investigation, Visualization. **N. Casati:** Conceptualization, Methodology, Resources, Writing – review & editing. **F. Gozzo:** Conceptualization, Data curation, Formal analysis, Investigation, Methodology, Supervision, Validation, Writing – original draft, Writing – review & editing.

## Declaration of Competing Interest

The authors have no pertinent financial or non-financial conflicts of interest to report. Nevertheless, they wish to disclose the following information that could be viewed as potential competing interests:

Nicola Casati leads the Swiss Light Source Materials Science beamline at the Paul Scherrer Institute, which is the largest national institute of applied research committed to support industrial applications based on the use of synchrotron radiation.

Mathilde Reinle-Schmitt, Fanny N. Costa, Mickael Morin and Fabia Gozzo are employed by Excelsus Structural Solutions (Swiss) AG, which is a spin-off company of the Paul Scherrer Institute that provides synchrotron radiation based analytical services to the industry.

Dubravka Šišak Jung is an employee of DECTRIS, a company which develops and manufactures detectors.

## Data availability

Data will be made available on request.

## Acknowledgements

The authors express their sincere appreciation to Michael Wörle, the head of the Small Molecule Crystallography Center (SMoCC) at the Swiss Federal Institute of Technology in Zurich (ETHZ), who graciously conducted high-resolution lab-XRPD measurements on the atorvastatin trihydrate powder. Special thanks are extended to Arnaud Grandeury, a distinguished scientist at Novartis Pharma in Basel, Switzerland, for providing the cinnarizine powder and engaging in insightful discussions.

Furthermore, the authors would like to acknowledge the invaluable support of the ANAXAM team for their assistance in testing pharmaceutical compounds using their optimized high-throughput system, along with their contributions to open and constructive discussions.

NC is grateful to Jarkko Stenman for the fruitful discussions, challenges and competent feedback during the development and optimization of the SLS high-throughput system and to Michael Lange for its technical development of the system.

Lastly, the authors extend their gratitude to Julie Stoll, a student at the *Centre d'Enseignement Professionnel de Vevey (CEPV)*, for her generous contribution to the cartoon featured in Fig. 2 (right).

## References

Abdellatief, M., Najdawi, M.A., Momani, Y., Aljamal, B., Abbadi, A., Harfouche, M., Paolucci, G., 2022. Operational status of the X-ray powder diffraction beamline at the SESAME synchrotron. J. Synchrotron Radiat. 29, 532–539. https://doi.org/10.1107/S1600577521012820.

Artioli, 2015. Powder diffraction and synchrotron radiation. In: Mobilio, S., Boscherini, F., Meneghini, C. (Eds.), Synchrotron Radiation. Springer, Berlin, Heidelberg. https://doi.org/10.1007/978-3-642-55315-8.

Bergamaschi, A., Cervellino, A., Dinapoli, R., Gozzo, F., Henrich, B., Johnson, I., Kraft, P., Mozzanica, A., Schmitt, B., Shi, X., 2010. The MYTHEN detector for X-ray powder diffraction experiments at the Swiss Light Source. J. Synchrotron Radiat. 17, 653–668. https://doi.org/10.1107/S0909049510026051.

Bernstein, J., Reutzel-Edens, S.M., 2019. Powder Diffraction and Pharmaceuticals in: International Tables for Crystallography, H, 7.5, pp. 773–777. https://onlinelibrary.wiley.com/iucr/itc/Ha/ch7o5v0001/ch7o5.pdf (accessed 13 October 2023).

Billinge, S.J.L., 2015. Atomic pair distribution function: a revolution in the characterization of nanostructured pharmaceuticals. Nanomedicine 10 (16), 2473–2475. https://doi.org/10.2217/nnm.15.116.

Blake, D., 2023. Mars Science Laboratory - CheMin Instrument. https://www.nasa.gov/centers/ames/pdf/604996main_CheMin_fact_sheet.pdf (accessed 23 October 2023).

Bruker, A.X.S., 2016. TOPAS, V6.0. (Version 6.0) (Computer Software), Bruker AXS, Karlsruhe, Germany. https://www.bruker.com/fr/products-and-solutions/diffractometers-and-x-ray-microscopes/x-ray-diffractometers/diffrac-suite-software/diffrac-topas.html.

Byrn, S.R., Coates, D.A., Gushurst, K.S., Morrison, H.G., Park, A., Vlahova, P.I., Li, Z.J., Krzyzaniak, J.F., 2003. US patent WO 03/004470 A1 PCT/IB02/01796. https://patentimages.storage.googleapis.com/b1/ad/26/410debb2c84364/AU2002258092B2.pdf (accessed 23 October 2023).

Byrn, S.R., Zografi, G., Chen, X., 2017. X-ray powder diffraction. In: Solid-State Properties of Pharmaceutical Materials, First Edition. John Wiley & Sons, Inc., pp. 107–123. https://doi.org/10.1002/9781119264408

Coelho, A.A., Evans, J., Evans, I., Kern, A., Parsons, S., 2011. The TOPAS symbolic computation system. Powder Diffract. 26 (S1), S22–S25. https://doi.org/10.1154/1.3661087.

Debye, P., Scherrer, P., 1916. Interferenzen an regellos orientierten Teilchen im Röntgenlicht. In: Nachrichten von der Gesellschaft der Wissenschaften zu Göttingen, Mathematisch-Physikalische Klasse, pp. 1–15. http://eudml.org/doc/58947 (accessed 23 October 2023).

Degen, T., Sadki, M., Bron, E., König, U., Nénert, G., 2014. The HighScore suite. Powder Diffract. 29 (S2), S13–S18. https://doi.org/10.1017/S0885715614000840.

Dejoie, C., Coduri, M., Petitdemange, S., Giacobbe, C., Covacci, E., Grimaldi, O., Autran, P.-O., Mogodi, M.W., Šišak Jung, D., Fitch, A.N., 2018. Combining a nine-crystal multi-analyser stage with a two-dimensional detector for high-resolution powder X-ray diffraction. J. Appl. Crystallogr. 51, 1721–1733. https://doi.org/10.1107/S1600576718014589.

DeWitt, K., 2015. X-Ray Powder Diffraction Method Development and Validation for the Identification of Counterfeit Pharmaceuticals. Marshall University. https://www.marshall.edu/forensics/files/DeWitt-Kelsey-Research-Paper-08072015-Final.pdf (accessed 23 October 2023).

Ditzinger, F., Dejoie, C., Sisak Jung, D., Kuentz, M., 2019. Polyelectrolytes in Hot Melt Extrusion: acombined Solvent-based and Interacting Additive Technique for Solid Dispersions. Pharmaceutics. 11 (4), 174. https://doi.org/10.3390/pharmaceutics11040174.

Donath, T., Šišak Jung, D., Burian, M., Radicci, V., Zambon, P., Fitch, A.N., Dejoie, C., Zhang, B., Ruat, M., Hanfland, M., Kewish, C., van Riessen, G.A., Naumenko, D., Amenitsch, H., Bourenkov, G., Bricogne, G., Chari, A., Schulze-Briese, C., 2023. EIGER2 hybrid-photon-counting X-ray detectors for advanced synchrotron experiments. J. Synchrotron Radiat. 30, 723–738. https://doi.org/10.1107/S160057752300454X.

Filik, J., Ashton, A.W., Chang, P.C.Y., Chater, P.A., Day, S.J., Drakopoulos, M., Gerring, M.W., Hart, M.L., Magdysyuk, O.V., Michalik, S., Smith, A., Tang, C.C., Terrill, N.J., Wharmby, M.T., Wilhelm, H., 2017. Processing two-dimensional X-ray diffraction and small-angle scattering data in DAWN 2. J. Appl. Crystallogr. 50 (3), 959–966. https://doi.org/10.1107/S1600576717004708.

Gates-Rector, S., Blanton, T., 2019. The Powder Diffraction File: a quality materials characterization database. Powder Diffract. 34 (4), 352–360. https://doi.org/10.1017/S0885715619000812.

Giannini, C., Cervellino, A., Guagliardi, A., Gozzo, F., Zanchet, D., Rocha, T., Ladisa, M., 2007. A Debye function-based powder diffraction data analysis method.

Z. Kristallogr. Suppl. 26, 105–110. https://doi.org/10.1524/zkri.2007.2007.suppl_26.105.
Gozzo, F., 2018. The Power of Synchrotron X-Ray Powder Diffraction for the Characterization of Pharmaceuticals. Pharm. Technol. 42 (2), 18. https://cdn.sanity.io/files/0vv8moc6/pharmtech/2043961cbd898be74617e46315d03533069e73a3.pdf/PharmTech_NA_Feb2018.pdf (accessed 23 October 2023).
Grässlin, J., McCusker, L.B., Baerlocher, C., Gozzo, F., Schmitt, B., Lutterotti, L., 2013. Advances in exploiting preferred orientation in the structure analysis of polycrystalline materials. J. Appl. Crystallogr. 46, 173–180. https://doi.org/10.1107/S0021889812045943.
Halasz, I., Kimber, S.A.J., Beldon, P.J., Belenguer, A.M., Adams, F., Honkimäki, V., Nightingale, R.C., Dinnebier, R.E., Friscic, T., 2013a. In situ and real-time monitoring of mechanochemical milling reactions using synchrotron X-ray diffraction. Nat. Protoc. 8, 1718–1729. https://doi.org/10.1038/nprot.2013.100.
Halasz, I., Puškarić, A., Kimber, S.A.J., Beldon, P.J., Belenguer, A.M., Adams, F., Honkimäki, V., Dinnebier, R.E., Patel, B., Jones, W., Štrukil, V., Friščić, T., 2013b. Real-time in situ powder X-ray diffraction monitoring of mechanochemical synthesis of pharmaceutical cocrystals. Angew. Chem. Int. Ed. 52, 11538–11541. https://doi.org/10.1002/anie.201305928.
Hammersley, P.A., 1997. FIT2D: An Introduction and Overview. ESRF Internal Report, ESRF97HA02T. https://www.esrf.fr/computing/scientific/FIT2D/FIT2D_INTRO/fit2d.html (accessed 23 October 2023).
Hocine, S., VanPetegem, S., Frommherz, U., Tinti, G., Casati, N., Grolimund, D., Van Swygenhoven, H., 2020. Operando X-ray diffraction during laser 3D printing. Addit. Manuf. 34, 101194 https://doi.org/10.1016/j.mattod.2019.10.001.
Hodge, R., Kaduk, J., Gindhart, A., Blanton, T., 2020. Crystal structure of atorvastatin calcium trihydrate form I (Lipitor®), $(C_{33}H_{34}FN_2O_5)_2Ca(H_2O)_3$. Powder Diffract. 35 (2), 136–143. https://doi.org/10.1017/S0885715620000147.
Hull, A.W., 1917. A New Method of X-ray Crystal Analysis. Phys. Rev. 10, 661. https://doi.org/10.1103/PhysRev.10.661.
Ivanisevic, I., McClurg, R.B., Schields, P.J., 2010. Uses of X-Ray powder diffraction in the pharmaceutical industry. In: Gad, S.C. (Ed.), Pharmaceutical Sciences Encyclopedia: Drug Discovery, Development, and Manufacturing. John Wiley & Sons. https://doi.org/10.1002/9780470571224.pse414.
Jenkins, R., 2001. Landmarks in the development of powder diffraction instrumentation. J. Chem. Educ. 78 (5), 601. https://doi.org/10.1021/ed078p601.1.
Juhas, P., Davis, T., Farrow, C.L., Billinge, S.J.L., 2013. PDFgetX3: a rapid and highly automatable program for processing powder diffraction data into total scattering pair distribution functions. J. Appl. Crystallogr. 46, 560–566. https://doi.org/10.1107/S0021889813005190.
Leaps Innovation, 2023. The Application of "Quality Assurance" to Synchrotron Services, A focus forum to debate the application of "quality assurance" in the context of commercial synchrotron services, Berlin 2–3 March 2023. https://www.esrf.fr/home/Industry/industry-news/content-news/esrf-news-list/qsa-forum-2023-towards-quality-assurance-to-synchrotron-services.html.
Mouille, Y., Cotrait, M., Hospital, M., Marsau, P., 1975. Trans-Cinnamyl-1 diphénylméthyl-4 pipérazine (cinnarizine). Acta Crystallogr. B31, 1495–1496. https://doi.org/10.1107/S0567740875005523.
Musumeci, D., Hu, C., Ward, M.D., 2011. Anticounterfeit protection of pharmaceutical products with spatial mapping of X-ray-detectable barcodes and logos. Anal. Chem. 83 (19), 7444–7450. https://doi.org/10.1021/ac201570r.
Newman, J.A., Schmitt, P.D., Toth, S.J., Deng, F., Zhang, S., Simpson, G.J., 2015. Parts per million powder X-ray diffraction. Anal. Chem. 87 (21), 10950–10957. https://doi.org/10.1021/acs.analchem.5b02758.
Pawley, G.S., 1981. Unit-cell refinement from powder diffraction scans. J. Appl. Crystallogr. 14 (6), 357–361. https://doi.org/10.1107/S0021889881009618.
Petříček, V., Dušek, M., Palatinus, L., 2014. Materials crystallographic computing system JANA2006: general features. Z. Kristallogr. – Cryst. Mater. 229 (5), 345–352. https://doi.org/10.1515/zkri-2014-1737.
Prescher, C., Prakapenka, V.B., 2015. DIOPTAS: a program for reduction of two-dimensional X-ray diffraction data and data exploration. High Pressure Res. 35 (3), 223–230. https://doi.org/10.1080/08957959.2015.1059835.
Rodriguez, I., Gautam, R., Tinoco, A.D., 2021. Using X-ray diffraction techniques for biomimetic drug development, formulation, and polymorphic characterization. Biomimetics 6 (1), 1. https://doi.org/10.3390/biomimetics6010001.
Rukiah, M., Lefebvre, J., Hernandez, O., Van Beek, W., Serpelloni, M., 2005. Ab initio structure determination of the Γ form of D-sorbitol (D-glucitol) by powder synchrotron X-ray diffraction. CCDC 254343 (37), 766. https://doi.org/10.1107/S0021889804016206.
Šišak Jung, D., Baerlocher, Ch., McCusker, L.B., Yoshinari, T., Seebach, D., 2014. Solving the structures of light-atom compounds with powder charge flipping. J. Appl. Crystallogr. 47, 1569–1574. https://doi.org/10.1107/S1600576714016732.
Šišak Jung, D., Donath, T., Magdysyuk, O., Bednarcik, J., 2017. High energy X-ray applications: current status and new opportunities. Powder Diffract. 32 (S2), S22–S27. https://doi.org/10.1017/S0885715617001191.
Smith, J.H., Dann, S.E., Elsegood, M.R.J., Dale, S.H., Blatchford, C.G., 2005. α-Lactose monohydrate: a redetermination at 150 K. Acta Crystallogr. Sect. E: Struct. Rep. Online E61, o2499–o2501. https://doi.org/10.1107/S1600536805021367.
Spiliopoulou, M., Karavassili, F., Triandafillidis, D.-P., Valmas, A., Fili, S., Kosinas, C., Barlos, K., Barlos, K.K., Morin, M., Reinle-Schmitt, M.L., Gozzo, F., Margiolaki, I., 2021. New perspectives in macromolecular powder diffraction using single-photon-counting strip detectors: high-resolution structure of the pharmaceutical peptide octreotide. Acta Crystallogr. A77, 186–195. https://doi.org/10.1107/S2053273321001698.
Stolar, T., Lukin, S., Tireli, M., Sović, I., Karadeniz, B., Kereković, I., Matijašić, G., Gretić, M., Katančić, Z., Dejanović, I., di Michiel, M., Ivan Halasz, I., Krunoslav Užarević, K., 2019. Control of Pharmaceutical Cocrystal Polymorphism on various Scales by Mechanochemistry: transfer from the Laboratory batch to the Large-Scale Extrusion Processing. ACS Sustain. Chem. Eng. 7 (7), 7102–7110. https://doi.org/10.1021/acssuschemeng.9b00043.
Stone, K.H., Lapidus, S., Stephens, P.W., 2009. Implementation and use of robust refinement in powder diffraction in the presence of impurities. CCDC 735844. https://doi.org/10.1107/S0021889809008450.
Streamline project: New high-throughput X-ray powder diffraction system on ID31. https://www.esrf.fr/home/news/tech-talk/content-news/tech-talk/techtalk13.html, 2023 (accessed 23 October 2023).
Sundaralingam, M., Jensen, L.H., 1965. Refinement of the structure of salicylic acid. Acta Crystallogr. 18, 1053–1058. https://doi.org/10.1107/S0365110X65002517.
Terban, M.W., Billinge, S.J.L., 2022. Structural analysis of molecular materials using the pair distribution function. Chem. Rev. 122 (1), 1208–1272. https://doi.org/10.1021/acs.chemrev.1c00237.
Thakral, N.K., Zanon, R.L., Kelly, R.C., Thakral, S., 2018. Applications of powder X-Ray diffraction in small molecule pharmaceuticals: achievements and aspirations. J. Pharm. Sci. 107 (12), 2969–2982. https://doi.org/10.1016/j.xphs.2018.08.010.
Thomae, S.L.J., Prinz, N., Hartmann, T., Teck, M., Correll, S., Zobel, M., 2019. Pushing data quality for laboratory pair distribution function experiments. Rev. Sci. Instrum. 90 (4), 043905 https://doi.org/10.1063/1.5093714.
Toby, B.H., Von Dreele, R.B., 2013. GSAS-II: the genesis of a modern open-source all purpose crystallography software package. J. Appl. Crystallogr. 46, 544–549. https://doi.org/10.1107/S0021889813003531.
Vanmeert, F., De Nolf, W., De Meyer, S., Dik, J., Janssens, K., 2018. Macroscopic X-ray powder diffraction scanning, a new method for highly selective chemical imaging of works of art: instrument optimization. Anal. Chem. 90 (11), 6436–6444. https://doi.org/10.1021/acs.analchem.8b00240.
Vaughan, G.B.M., Baker, R., Barret, R., Bonnefoy, J., Buslaps, T., Checchia, S., Duran, D., Fihman, F., Got, P., Kieffer, J., Kimber, S.A.J., Martel, K., Morawe, C., Mottin, D., Papillon, E., Petitdemange, S., Vamvakeros, A., Vieux, J.-P., Di Michiel, M., 2020. ID15A at the ESRF – a beamline for high-speed operando X-ray diffraction, diffraction tomography, and total scattering. J. Synchrotron Radiat. 27, 515–528. https://doi.org/10.1107/S1600577519016813.
Willmott, P.R., Meister, D., Leake, S.J., Lange, M., Bergamaschi, A., Böge, M., Calvi, M., Cancellieri, C., Casati, N., Cervellino, A., Chen, Q., David, C., Flechsig, U., Gozzo, F., Henrich, B., Jäggi-Spielmann, S., Jakob, B., Kalichava, I., Karvinen, P., Krempasky, J., Lüdeke, A., Lüscher, R., Maag, S., Quitmann, C., Reinle-Schmitt, M.L., Schmidt, T., Schmitt, B., Streun, A., Vartiainen, I., Vitins, M., Wang, X., Wullschleger, R., 2013. The materials science beamline upgrade at the Swiss light source. J. Synchrotron Radiat. 20, 667–682. https://doi.org/10.1107/S0909049513018475.